Recent New Developments in Contact Mechanics

Authors:
P. Wriggers and K. Fischer,
Institut für Baumechanik und Numerische Mechanik, Universität Hannover
A. Rieger, Continental AG

Correspondence:
P. Wriggers
Institut für Baumechanik und Numerische Mechanik, Universität Hannover
Universität Hannover
Appelstr. 9a
30167 Hannover, Germany

Keywords:
contact, adaptive finite element method,
mortar method, thermo-mechanical contact

Abstract

During the last years considerable effort was devoted to better numerical treatment of contact problems. This fact is due to the growing computing power which lead to more and more sophistication and detailed technical models within engineering analysis. Due to the more precise modelling within the associated discretization process often unilateral constraints have to be considered. Hence better discretization techniques, especially for finite deformations, are needed to solve problems with contact constraints in an efficient and robust way. In this paper we will discuss some recently developed discretization schemes and algorithms for the treatment of contact constraints.

The presentation is split into two parts. The first one is devoted to discretization techniques for contact problems which fulfill the BB-condition needed for a stable contact discretization scheme. This leads to a discussion of weak enforcement of the contact constraint conditions which results in so-called mortar methods for linear and nonlinear problems. Here also special remarks are made with regard to efficient solution schemes which are based on a total gap vector at the contact interface.

The second part of the presentation is related to adaptive finite element methods for large deformation thermo-mechanical contact problems. Here a

special staggered scheme is developed in which different finite element meshes are combined to solve the thermo-mechanical contact problem. Based of the methodology of the Zienkiewicz, Zhu error indicators based on superconvergent patch recovery special error indicators are developed for the the mechanical and thermal part of the problem including the contact constraints. Furthermore an error indication in time is derived for the thermal heat conductance equation based on a time-space discretization which uses a continuous Galerkin scheme for the time integration. Using such integration algorithm one can derive again a error indicator by assuming superconvergent time points. This method is applied to solve an example with known analytical solution which allows the computation of efficiency indices. Here it can be shown that the developed adaptive time stepping scheme results in very good efficiency of the method.

For all parts, the basic theoretical basis is derived, algorithmic implications are discussed and explanatory examples are presented to show the properties of formulations when compared to existing ones.

1 Discretization for Non-matching Meshes

By using general mesh generators, unstructured meshes can be constructed in which nodes in the contact interface do not assume the same coordinates, see Figure 1. Then the formulations discussed above can no longer be applied, even in the geometrically linear case.

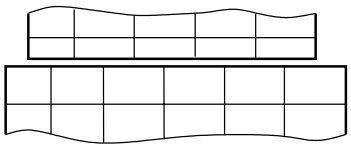

Figure 1: Contact discretization with non-matching meshes.

Methods for connecting finite element domains with non-matching grids (see Figure 1) are frequently used for parallel computations. Such formulations have different origins, and hence have also received special names. A commonly used approach is the mortar method. However, other methods like the NITSCHE method exist. The formulations are designed in such a way that they fulfil the BB conditions, also called *inf-sup* conditions, and hence lead to a stable discretization. For a good literature overview and the underlying mathematical theory we recommend (Wohlmuth, 2000a). There are also approaches which were developed in the engineering literature, e.g. see (Simo et al., 1985) or (Papadopoulos and Taylor, 1992). Here either a LAGRANGE or penalty formulation was applied. Treatments which include friction can also be found in (Krause and Wohlmuth, 2001) or (McDevitt and Laursen, 2000).

1.1 Mortar method

The mortar method is a special technique to enforce contact constraints in the discretized system for non-matching meshes. The method is based on a LAGRANGE multiplier formulation in which special interpolation functions are used to discretize the LAGRANGE multiplier in the contact interface. The method which leads to a non-conforming approach is based on direct enforcements of the constraints, and hence is equivalent to the direct constraint elimination. This method is described in (Bernadi et al., 1994) and (Wohlmuth, 2000a). It leads to a positive definite system of equations. Another method is related to the weak enforcement of the constraints by applying the LAGRANGE multiplier method. In the mortar literature different interpolations for the LAGRANGE multipliers are introduced. In general, one can use linear, quadratic or even higher order interpolation functions. However, due to the weak formulation of the constraints, mathematical conditions like the BABUSKA–BREZZI condition have to be fulfilled in order to achieve a stable discretization scheme; for details, see (El-Abbasi and Bathe, 2001) for a numerical and (Wohlmuth, 2000a) for a theoretical approach.

Several techniques can be followed to define the contact surface. One is based on the use of an intermediate contact surface as the reference surface and to define the LAGRANGE multipliers on this surface. This intermediate contact surface C defines the *mortar* side in the interface. Early formulations can be found in (Simo et al., 1985). Lately mortar discretizations, based on the intermediate surface, have been developed in (McDevitt and Laursen, 2000) or (Rebel et al., 2000).

Another choice is made in the mathematical literature, e.g. see (Wohlmuth, 2000b) and (Krause and Wohlmuth, 2001), which is based on the assumption that the mortar side is one of the surfaces of the bodies in the contact interface which would, for example, in our notation be the master surface. In (Wohlmuth, 2000b) it was shown that such formulation with the appropriate interpolation functions for the LAGRANGE multipliers fulfils the BB condition. Furthermore, the LAGRANGE multiplier interpolation can be constructed in such a way that the locality of the support of the nodal basis functions is preserved. Hence this formulation leads from a mathematical viewpoint to a stable discretization, and yields a good approximation of the contact stresses.

1.2 Contact Kinematics

Within contact formulations the Mortar method enables the connection of unstructured meshes using a LAGRANGE multiplier formulation. The idea is to variationally project the displacements from one contacting continuum to the next, directly by transfer operators, see [1]. In this description, the LAGRANGE multipliers are associated to the so called non-mortar surface. The

other contact surface is the mortar surface. The non-mortar surface gives the tangential $\bar{\mathbf{a}}_\alpha^{nm} = \frac{d}{d\,\xi^{nm\,\alpha}}\,\mathbf{x}^{nm}\,(\,\bar{\boldsymbol{\xi}}^{nm},\,t\,)$ and normal vector

$$\bar{\mathbf{n}}^{nm} := \frac{\bar{\mathbf{a}}_1^{nm} \times \bar{\mathbf{a}}_2^{nm}}{\parallel\, \bar{\mathbf{a}}_1^{nm} \times \bar{\mathbf{a}}_2^{nm}\, \parallel} \tag{1}$$

onto which the distance between the two surfaces is projected. This distance is the gap between one point on the mortar and another point on the non-mortar surface. The projection in normal direction is called the normal gap

$$g_N := \left[\,\mathbf{x}^m - \mathbf{x}^{nm}\,(\,\bar{\boldsymbol{\xi}}^{nm},\,t\,)\right] \cdot \bar{\mathbf{n}}^{nm} \qquad . \tag{2}$$

The tangential gap $g_T = g_{T\,\alpha}\,\bar{\mathbf{a}}^{nm\,\alpha}$ with

$$g_{T\,\alpha} = \int_{t_0}^{t} \left\{\left[\dot{\mathbf{x}}^m - \dot{\mathbf{x}}^{nm}(\,\bar{\boldsymbol{\xi}}^{nm},\,t\,)\right] \cdot \bar{\mathbf{a}}_\alpha^{nm} + g_N \bar{\mathbf{n}}^{nm} \dot{\bar{\mathbf{a}}}_\alpha^{nm}\right\}\,dt \tag{3}$$

represents the relative displacement of the two contact points projected in tangential direction. In case of stick there is no relative motion, so $g_T = 0$. In case of sliding g_T is expressed by the time-dependent change of the contact points and the tangential vector.

1.3 Weak Formulation

The contact virtual work contains the contact constraints using a LAGRANGE multiplier formulation

$$\Pi_c = \int \left(\lambda_N \cdot g_N + \boldsymbol{\lambda}_T \cdot \mathbf{g}_T\right)\,d\Gamma_c^{nm} \qquad , \tag{4}$$

where the non-mortar surface gives the integration area. The multipliers represent the contact pressure (λ_N) and the tangential stress ($\boldsymbol{\lambda}_T$). The weak form is decomposed into a formulation for stick

$$C_c^{\text{stick}} = \int \left(\delta\lambda_N \cdot g_N + \lambda_N \cdot \delta g_N + \delta\boldsymbol{\lambda}_T \cdot \mathbf{g}_T + \boldsymbol{\lambda}_T \cdot \delta\mathbf{g}_T\right)\,d\Gamma_c^{nm} \tag{5}$$

and another one for slip

$$C_c^{\text{slip}} = \int \left(\delta\lambda_N \cdot g_N + \lambda_N \cdot \delta g_N + \boldsymbol{t}_T \cdot \delta\mathbf{g}_T\right)\,d\Gamma_c^{nm} \qquad . \tag{6}$$

For sliding $\boldsymbol{\lambda}_T$ is replaced by the tangential stress $\mathbf{t}_T$ which is calculated from the constitutive law for frictional slip; therefore it has not to be varied.

We observe that the integration along the non-mortar side using the same shape functions for the displacement field and the LAGRANGE multipliers yields a mass matrix. Assembly of all n_c terms on both sides of C_c

$$\delta\boldsymbol{\lambda}_N^T\,(\,\boldsymbol{M}^2\,\boldsymbol{u}^2 - \boldsymbol{M}^1\,\boldsymbol{u}^1\,) = 0\,, \tag{7}$$

from which we can eliminate the displacements $\boldsymbol{u}^2$ on the non-mortar side by

$$\boldsymbol{u}^2 = \left(\boldsymbol{M}^2\right)^{-1} \boldsymbol{M}^1 \, \boldsymbol{u}^1 \, . \tag{8}$$

In (7) we have computed matrix $\boldsymbol{M}^1$ segment-wise, e.g. $\boldsymbol{M}^1$ follows from an integration by dividing a segment c into i and j on the mortar side. This integration can be performed exactly or by using a quadrature rule. For the linear interpolation with straight segments, a two-point GAUSS quadrature is sufficient, and yields an exact integration. For higher order isoparametric interpolations an exact integration is more involved, since the contact surfaces can be curved, which leads to non-constant JACOBIANS.

Since $\boldsymbol{M}^2$ is not a diagonal matrix the influence of one displacement u_J^1 is coupled with all displacements $\boldsymbol{u}^2$. The same is true when the LAGRANGE multipliers are kept within the formulation. Also, there the locality of the nodal basis function is lost.

1.4 Special discretization

The exact integration over the discretized non-mortar surface is only possible in the overlapping region (see figure 2 left) of all three interpolation functions. Note that they are C_1-continuous in such a segment. As integration rule a two GAUSS-point scheme is used in each of the segments which is sufficient for the multiplication of two linear shape functions. The mortar element

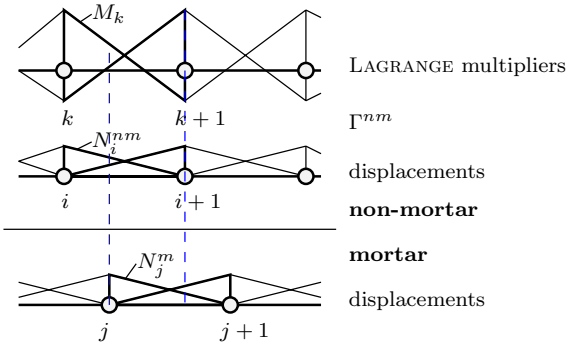

Figure 2: Mortar element description

itself can be described by the values, given in figure 2. The deformations and the LAGRANGE multipliers are discretized functions depending on the surface coordinate ξ. The shape functions for the displacements are the standard linear interpolation functions.

$$M_1^{nm}\left(\xi^{nm}\right) = 2 \, - \, 3\,\xi^{nm} \qquad M_2^{nm}\left(\xi^{nm}\right) = -1 \, + \, 3\,\xi^{nm} \tag{9}$$

The interpolation functions for the LAGRANGE multipliers M_1 and M_2 are defining a dual, orthogonal, base to the standard interpolation functions.

Due to the orthogonality property, using the shape functions (2), an assembled matrix form of the weak contact constraint equation is given by

$$\delta \boldsymbol{\lambda}_N^T \left(\boldsymbol{D}^2 \, \boldsymbol{u}^2 - \boldsymbol{M}^1 \, \boldsymbol{u}^1 \right) = 0 \,, \tag{10}$$

instead of (7). Hence the elimination (8) can now be expressed as

$$\boldsymbol{u}^2 = \left(\boldsymbol{D}^2 \right)^{-1} \, \boldsymbol{M}^1 \, \boldsymbol{u}^1 \,, \tag{11}$$

where $\boldsymbol{D}^2$ is a diagonal matrix. This leads to a contact interpolation with a local support, which is computationally more efficient.

1.5 Example

A frictional contact problem between a block and a rigid plane shows that the LAGRANGE multipliers correlate well with the stresses, see figure 3. The block is loaded in horizontal and vertical direction with different uniform loads. It is bent at the mortar element leftmost in vertical and horizontal, at the element rightmost in vertical direction. Sliding and sticking elements can be distinguished.

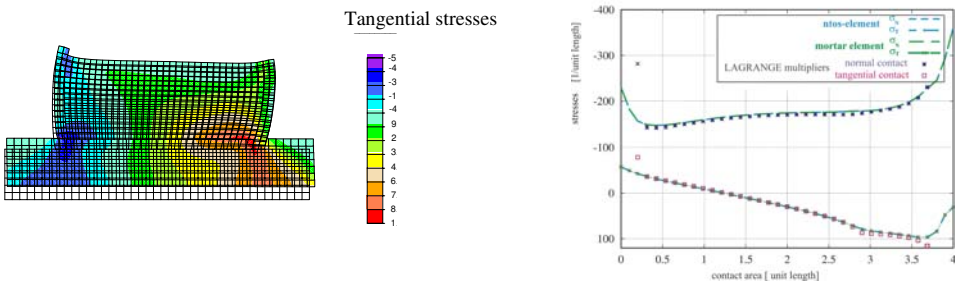

Figure 3: Frictional contact problem between a block and a rigid plane

2 Adaptive thermomechanical contact

In contact problems the contact interface is not known a priori. Hence the finite element mesh cannot be easily adjusted by hand. Due to that it is desirable to use adaptive techniques in contact mechanics. The objective of adaptive techniques is to obtain a discretization which is optimal in the sense that the computational costs involved are minimal under the constraint that the error in the finite element solution is below a certain limit. Error estimators which are most frequently used in solid mechanics for elastic problems are

based on residual computations, see e.g. (Johnson and Hansbo, 1992) or on superconvergence properties (ZZ-approach), see e.g. (Zienkiewicz and Zhu, 1987). To make the ZZ-approach applicable to the thermomechanical coupled contact problem, a special projection scheme must be applied since the stress field and heat flux are only C^0-continuous across the interface. Furthermore, specific constraints and continuity conditions have to be taken into account to improve the gradient recovery on the contact boundary.

2.1 Boundary value problem

In order to state the governing equations of the thermomechanical coupled contact problem, let us first consider two elastic bodies.

Balance of Momentum and Conservation of Energy. The local system of partial differential equations governing the coupled thermomechanical Initial-Boundary-Value-Problem (IBVP) referred to the current configuration is stated as

$$div\,\boldsymbol{\sigma} + \rho\mathbf{b} = \mathbf{0} \qquad -div\,\mathbf{q} = \rho c\dot{\vartheta}\,, \tag{12}$$

$\boldsymbol{\sigma} = \boldsymbol{\sigma}^T$ denotes the symmetric CAUCHY stress tensor, $\mathbf{b}$ the specific body force vector and ρ the current density, respectively. c denotes the specific heat capacity and ϑ defines a relative temperature according to $\vartheta := \theta - \theta_0$ with an arbitrary and constant reference temperature θ_0. $\mathbf{q}$ the heat flux. In this presentation we consider only quasistatic processes with purely elastic material response. Furthermore, it is assumed that heat sources inside the body do not exist. With $\mathbf{F}$ denoting the deformation gradient and the definition of the finite strain rate tensor $\mathbf{d} := sym\{\dot{\mathbf{F}} \cdot \mathbf{F}^{-1}\}$ In the following considerations we assumed that only moderate strain rates occur and $\frac{3\alpha K}{J}\theta tr\mathbf{d} << \rho c\dot{\vartheta}$ holds. Where K denotes the bulk modulus, α is the thermal expansion coefficient and $J = det\mathbf{F}$ is the Jacobian.

Boundary conditions and Initial conditions. The boundary $\partial\mathcal{B}^\alpha$ of a body $\mathcal{B}^\alpha$ consists of a part $\partial\mathcal{B}^\alpha_\sigma \subset \partial\mathcal{B}^\alpha$ with prescribed surface loads, a part $\partial\mathcal{B}^\alpha_u \subset \partial\mathcal{B}^\alpha$ with prescribed displacements and a part $\partial\mathcal{B}^\alpha_c \subset \partial\mathcal{B}^\alpha$ where the two bodies $\mathcal{B}^m$ and $\mathcal{B}^s$ come into contact. Furthermore we have a subdomain $\partial\mathcal{B}_\vartheta \subset \partial\mathcal{B}^\alpha$ with a prescribed temperature and the subset $\partial\mathcal{B}_q \subset \partial\mathcal{B}^\alpha$ where the outward normal heat flux is given.

In order to specify the thermomechanical process we additionally assume initial conditions for the displacement and the thermal field.

Contact Kinematics. Within the *master-slave* concept we define $\partial\mathcal{B}^m$ as the master surface and $\partial\mathcal{B}^s$ as the slave surface. When assuming that the contact boundary describes, at least locally, a convex region, then we can relate to

every point $\mathbf{x}^s$ on $\partial\mathcal{B}^s$ a point $\bar{\mathbf{x}}^m = \mathbf{x}^m(\bar{\xi}^\alpha)$ on $\partial\mathcal{B}^m$ via the minimal distance problem, see section 1.2. At the minimum distance point we can define the covariant base vectors of the master surface $\mathbf{a}_\alpha^m$ and the normal vector $\bar{\mathbf{n}}^m = \bar{\mathbf{n}}$. Furthermore we set $\bar{\mathbf{a}}_\alpha^m = \bar{\mathbf{a}}_\alpha$ omitting the superscript m. Once the point $\bar{\mathbf{x}}^m$ is known, we can write the geometrical contact constraint inequality which permits penetration of one body into the other $g_N := (\mathbf{x}^s - \bar{\mathbf{x}}^m) \cdot \bar{\mathbf{n}} \geq 0$. In view of the penalty formulation which will be applied to solve the contact problem, we introduce a penetration function since the method allows a small penetration in $\partial\mathcal{B}_c$:

$$g_N^- = \begin{cases} (\mathbf{x}^s - \bar{\mathbf{x}}^m) \cdot \bar{\mathbf{n}} & \text{if } (\mathbf{x}^s - \bar{\mathbf{x}}^m) \cdot \bar{\mathbf{n}} < 0 \\ 0 & \text{otherwise .} \end{cases} \tag{13}$$

In order to formulate the constitutive relation for the evolution of the tangential slip, we have to compute the tangential relative slip rate between the two bodies, see 1.2. For details of contact kinematics and the related linearizations see (Wriggers, 2002).

Thermoelastic Constitutive Equations for Finite Deformations. Although the constitutive behaviour of the bodies $\mathcal{B}^\alpha$ coming into contact does not affect the solution algorithm described here, we like to introduce some simple constitutive equation for finite thermoelasticity.
The simplest constitutive model for isotropic hyperelasticity, being polyconvex, is a compressible Neo–HOOKian model where the CAUCHY stress is given by

$$\boldsymbol{\sigma} = \frac{K}{J}\, ln J\, \mathbf{1} + \frac{\mu}{J}\, dev\, \overline{\mathbf{b}} \tag{14}$$

with the bulk modulus K, the shear modulus μ, the jacobian J and the second order identity tensor $\mathbf{1}$. The deviatoric stress in (14) is given in terms of the deviatoric part $\bar{\mathbf{b}}$ of the left CAUCHY-GREEN tensor $\mathbf{b} = \mathbf{F} \cdot \mathbf{F}^T$ (Miehe, 1988). With the definition $\overline{\mathbf{b}} := J^{-\frac{2}{3}}\, \mathbf{b}$. In order to construct a constitutive relation describing the finite thermal deformation we apply a multiplicative split of the volumetric deformation J into a thermal and stress free part J_ϑ, and an elastic part J_e which induces stresses: $J = J_e\, J_\vartheta$. The exponential constitutive law $J_\vartheta = e^{3\,\alpha\,\vartheta}$ is adopted for the thermal expansion where α denotes the thermal expansion coefficient.
In the case of isotropic heat conduction the heat flow $\mathbf{q}$ is given by the well known FOURIER law $\mathbf{q} = -k\, grad\, \vartheta$ with the positive thermal conductivity constant k. Note that the relation is nonlinear since $grad\,(\cdot)$ refers to the deformed configuration.
To complete the formulation, we have to introduce constitutive equations in the contact interface $\partial\mathcal{B}_c$. Within the penalty formulation the normal contact pressure is given by $t_N = \epsilon_N g_N^-$. The penalty parameter $\epsilon_N > 0$ can be interpreted as the stiffness in a very simple spring model.

The key idea in the constitutive model for the tangential stresses $t_{T\alpha}$ is a split of the tangential slip $\mathbf{g}_T$ into an elastic (stick) part $\mathbf{g}_T^e$ and an plastic (slip) part $\mathbf{g}_T^s$ (Wriggers, 1987) or (Wriggers, 2002): $\mathbf{g}_T := \mathbf{g}_T^e + \mathbf{g}_T^s$. This way the stick part still includes micro displacements which apart from a physical interpretation can also be called a regularization. Hence, we assume a very simple model related to a linear spring which yields $\mathbf{t}_T = c_T \mathbf{g}_T^e$, where c_T is a material parameter. The tangential plastic slip $\mathbf{g}_T^s$ is governed by a constitutive evolution equation which can be derived by using standard concepts of the theory of elastoplasticity. Within this framework we can formulate a plastic slip function $f_s(t_N, \mathbf{t}_T)$ for a given contact pressure t_N. Frictional sliding can be determined with a slip criterion which we can specialized by the classical COULOMB's model $f_s \equiv ||\mathbf{t}_T|| - \mu\, t_N \leq 0$, where μ is the friction coefficient. The evolution of the frictional slip can be stated in the form of a non–associated rule in the contact zone as $\dot{\mathbf{g}}_T^s = -\lambda \frac{\partial f_s}{\partial \mathbf{t}_T}$ if $f_s = 0$ with the tangential slip rate $\dot{\mathbf{g}}_T^s$, see 1.2.
For our purposes we apply a simple model for the heat flux across the contact interface (Wriggers and Miehe, 1994) (de Saracibar, 1998) in terms of the contact pressure t_N, the VICKERS hardness H_v , a resistance coefficient h_{c0} and a material constant ϵ of the form

$$q_{hc}(\mathbf{x}, t) := h_{c_0} \left(\frac{t_N}{H_v} \right)^{\epsilon} g_\theta(\mathbf{x}, t) \tag{15}$$

$g_\theta := \vartheta^s - \vartheta^m$ denotes the thermal gap.
In of friction the resulting outward normal heat flux q on $\partial\mathcal{B}_c^s$ and $\partial\mathcal{B}_c^m$ is the sum of the conducted heat flux q_{hc} and a heat source due to the frictional dissipation d_{fric} :

$$q^{(i)} = q_{hc}^{(i)} - \frac{1}{2}\, d_{fric} \qquad \text{on} \quad \partial\mathcal{B}_c^i \quad (i = s, m) \tag{16}$$

The frictional dissipation is given in terms of the plastic slip rate $\dot{\xi}^{s\,\alpha}$ and the tangential stress vector $\mathbf{t}_T$ by

$$d_{fric} = -\dot{\xi}^{s\,\alpha}\, \mathbf{a}_\alpha \cdot \mathbf{t}_T = -\dot{\xi}^{s\,\alpha}\, t_{T\alpha} \tag{17}$$

Variational Form of the IBVP. The weak form of the balance of momentum and the conservation of energy (12) can be achieved by taking the L_2 inner products with any test functions $\delta\mathbf{u}^\alpha \in \mathcal{V}_M$ and $\delta\vartheta^\alpha \in \mathcal{V}_\vartheta$ out of the usual admissible variation spaces $\mathcal{V}_M$ and $\mathcal{V}_\vartheta$, respectively. Due to the fact that the non-penetration condition is given by an inequality, we subsequently achieve a variational inequality (Wriggers, 2002). One of he most common approaches to solve this problem is an active-set strategy (Luenberger, 1984), which also

will be employed within this paper, combined with a penalty method. This leads to an expression of the form

$$\begin{aligned} G^M &= \sum_{\alpha=m,s} G_i^{\alpha M} - \lambda^M f^{\alpha M} + G_c^M = 0 \\ G^\vartheta &= \sum_{\alpha=m,s} G_i^{\alpha\,\vartheta} - \lambda^\vartheta f^{\alpha\vartheta} + G_c^\vartheta = 0 \end{aligned} \tag{18}$$

where the variational balance of momentum G_M and the variational conservation of energy G_ϑ, respectively, can be split in internal parts $(\,\cdot\,)_i$, parts $(\,\cdot\,)_c$ which are associated with the contact interface and load parts f. The parameters λ^M, λ^ϑ where introduced to allow scaling of the applied loads. The explicit expressions in (18) are given by

$$G_i^{\alpha M} = \int_{\mathcal{B}^\alpha} (grad\,\delta\mathbf{u} : \boldsymbol{\sigma} - \delta\mathbf{u}\cdot\rho\mathbf{b})\,dv \qquad f^{\alpha M} = \int_{\partial\mathcal{B}^\alpha_\sigma} \delta\mathbf{u}\cdot\hat{\mathbf{t}}\,da \tag{19}$$

$$G_i^{\alpha\,\vartheta} = \int_{\mathcal{B}^\alpha} (-grad\,\delta\vartheta\cdot\mathbf{q} + \delta\vartheta\rho\,c\,\dot{\vartheta})\;dv \qquad f^{\alpha\vartheta} = \int_{\partial\mathcal{B}^\alpha_q} -\delta\vartheta\,\hat{q}_n\,da \tag{20}$$

The contact terms in (18) take the form

$$G_c^M = \int_{\partial\mathcal{B}_c} (t_N\,\delta g_N - t_{T\alpha}\,\delta\bar{\xi}^\alpha)\,da \qquad G_c^\vartheta = \int_{\partial\mathcal{B}_c} (q_{hc}\,\delta g_\theta + \dot{\bar{\xi}}^{s\alpha}\,t_{T\alpha}\,\delta\theta_G)\,da \tag{21}$$

with $\theta_G := \frac{1}{2}\,(\,\vartheta^s + \vartheta^m\,)$ defining the mean interfacial temperature.

2.2 Discretization

In order to discretize the nonlinear variational problem (18) we use the standard finite-element approach. Details on the matrix formulation of the residual and tangent operators which are needed to apply NEWTON's incremental solution scheme can be found in (Wriggers and Miehe, 1994) or (de Saracibar, 1998).

For our purposes we state a time-space finite element formulation where the time axis $t \in [0, T]$ is approximated by means of a finite-element ansatz. The key idea of this approach was initially proposed in (Hulme, 1972) for nonlinear initial boundary value problems and has been applied for nonlinear elastodynamics in (Betsch and Steinmann, 2001). For the considered thermo-elastic contact problem the formulation has to be modified in a sufficient way. With the definition of the variable z

$$z = \int_{\mathcal{B}_t} \overset{*}{\vartheta}\,\rho\,c\,\vartheta\,dv \tag{22}$$

and the function $H(z)$

$$H(z) = \int_{\mathcal{B}_t} grad\, \overset{*}{\vartheta}\, \cdot(-\mathbf{q})\, dv - \lambda^{\vartheta} \int_{\partial\mathcal{B}_{tq}} \overset{*}{\vartheta}\, (-\hat{q}_N)\, da + \int_{\partial\mathcal{B}_c} q_{hc}\, \overset{*}{g}_{\theta}\, da \qquad (23)$$

the variational equation G^{ϑ} in (18) can be rewritten as a ordinary first order differential equation:

$$\dot{z} + H(z) = 0 \quad \text{for} \quad 0 < t < T \qquad \text{with} \quad z(0) = z_0 \qquad (24)$$

The infinitesimal frictional work dW_{fric} in (22) is defined according to the frictional dissipation in (17).
Next we state the time discretization of (24). In standard fashion we introduce a partition $0 = t_0 < t_1 < ... < t_n = T$ of $\mathcal{I} = [0, T]$ into time intervals $\mathcal{I}_n := (t_{n-1}, t_n)$ of length $h_\tau = t_n - t_{n-1}$. Within the sub-interval $\mathcal{I}_n$ the transformation $\alpha(t) = \frac{t - t_{n-1}}{h_\tau}$ is introduced defining the parametric mapping $\alpha \in [\![:= (0, 1) \rightarrow \mathcal{I}_n$ to a master element with the local coordinate α. With $dt = h_\tau\, d\alpha$ and the abbreviation $d(\cdot)/d\alpha = (\cdot)'$ the finite element formulation of the initial value problem in (24) now reads

$$\int_0^1 \delta z^h\, [z^{h\,\prime} + h_\tau\, H(z^h)]\, d\alpha \;=\; 0 \qquad \text{with} \quad z^h(0) = z_{n-1} \qquad (25)$$

Here z_{n-1} denotes the algorithmic approximation to z at time t_{n-1} from the previous time step. The trial functions z are represented by the polynomial interpolation where the nodal shape functions $N_J(\alpha)$ coincide with LAGRANGE polynomials of degree k such that $N_I(\alpha_J) = \delta_{IJ}$ and $z_J = z^h(\alpha_J)$ are the nodal values of z^h. Accordingly, the global approximation to z remains continuous. The test functions δz are represented by a reduced polynomial ansatz with reduced shape functions $\tilde{N}_I(\alpha)$ of polynomial order $k - 1$. Inserting the chosen interpolations into (25) yields to the algebraic equation system

$$\sum_{I=1}^{k} \sum_{J=1}^{k+1} \int_0^1 \tilde{N}_I N_J^{'}\, d\alpha\; z_J \;+\; \sum_{I=1}^{k} h_\tau \int_0^1 \tilde{N}_I H(z)\, d\alpha \;=\; 0 \qquad (26)$$

For our purposes we choose a polynomial degree of $k = 1$, hence the shape functions are given by $N_1(\alpha) = 1 - \alpha\,, N_2(\alpha) = \alpha\,, \tilde{N}_1 = 1$ and eqn. (26) reduces to

$$z_2 - z_1 + h_\tau \int_0^1 H(z^h)\, d\alpha = 0 \qquad (27)$$

The integral in (27) is evaluated using a two point GAUSS integration.

2.3 Staggered solution scheme

The key idea to solve the fully coupled equation system efficiently is the introduction of an additive operator split. It was shown in (Armero and Simo, 1992) that only an isentropic operator split preserves the contractivity property of the full problem leading to an unconditionally stable product formula staggered algorithm. Regardless of this fact, we apply the classical isothermal operator split obeying a staggered time integration algorithm in which the mechanical sub–problem without heat conduction at constant temperature is solved first, followed by a thermal heat conduction problem at a fixed mechanical configuration. Moreover we extend this solution algorithm to a separate and independent spatial discretization of the thermal and the mechanical sub domain to account for the different types of partial differential equations in the thermal and mechanical phase. Within this scheme *a-posteriori* error estimates control the grid density of both sub domains independently. Thus, each mesh can be optimized on its own. The coupling between the two grids is established by the formal projection operators

$$\begin{aligned} \boldsymbol{P}^{u}_{s\to t} &= \{\mathbf{u}_t\,,\,\bar{\xi}^{s}_{t-1}\}_{\Omega^s} \;\to\; \{\mathbf{u}_t\,,\,\bar{\xi}^{s}_{t-1}\}_{\Omega^t} \\ \boldsymbol{P}^{\vartheta}_{t\to s} &= \{\vartheta_t\}_{\Omega^t} \;\to\; \{\vartheta_t\}_{\Omega^s} \end{aligned} \tag{28}$$

which project the primal variables $\mathbf{u}$ and ϑ from the source-domain Ω^s to the target-domain Ω^t and vice versa.

Projection of Primal Variables. In what follows we denote a data delivering mesh as the source mesh Ω^s. A domain on which this data is projected on is called the target mesh Ω^t.
An arbitrary primal variable $\boldsymbol{\Phi}$ in the source domain Ω^s and the target domain Ω^t is given by

$$\boldsymbol{\phi}^{s,t}(\mathbf{x}) = \sum_{I=1}^{n^{s,t}} N_I(\mathbf{x})\boldsymbol{\Phi}^{s,t}_I \;\text{ in }\; \Omega^s \tag{29}$$

with the shape functions N_I, the nodal values $\boldsymbol{\Phi}_I$ and the number of nodal points n^s and n^t. The projection of the source variables on to the target grid can be formulated as a minimization problem: Find nodal values n^t that minimizes the error norm W

$$W := \int_\Omega F[\boldsymbol{\phi}^q(\mathbf{x}) - \boldsymbol{\phi}^z(\mathbf{x})]\; d\Omega \to MIN \tag{30}$$

where F is a specific function. Commonly a $L2$-norm of the form is used. Here we choose a cheaper error norm of the form

$$W = \int_\Omega \lambda(\mathbf{x})\; ||\boldsymbol{\phi}^s(\mathbf{x}) - \boldsymbol{\phi}^t(\mathbf{x})||\; d\Omega$$

with the weighting function $\lambda(\mathbf{x}) := \frac{1}{n^t}\sum_{K=1}^{n^t}\delta(\mathbf{x}-\mathbf{x}_K^t)$. With this the minimization problem (30) reads

$$W = \sum_{K=1}^{n^t} ||\boldsymbol{\phi}^s(\mathbf{x}_K^t) - \boldsymbol{\Phi}_K^t|| \rightarrow MIN \tag{31}$$

It leads to a cheap formula to calculate the unknown nodal values $\boldsymbol{\Phi}_K^t$ of the target grid.

In problems with frictional heating the dissipation power has to be known on the thermal mesh. For this one needs t_T and $\dot{\xi}^g$ which are also not known on the thermal mesh. However these values can be projected with the procedure described above since the frictional slip is known at time t.

2.4 Spatial error estimation

Within this presentation we consider the ZZ-approach. It is well known that the quality of the recovered gradients is inaccurate at or near boundaries compared to interior points. Motivated by the method presented by (Wiberg et al., 1998) for the gradient recovery in patches including DIRICHLET or NEUMANN boundaries, we develop a projection method with the aim of obtaining improved recovered gradients on the contact boundary, see below.
Note that since the considered transient problem is path- and time-dependent, also time discretization errors occur depending on the amount of time steps used to integrate the governing equations. In this study we formulate an time discretization error indicator based on the superconvergent projection method. Let us define the following L_2-norm

$$\| \nabla \mathbf{e}_v \|^2_{L2(\mathcal{B}_v)} = \int_{\mathcal{B}_v} (\mathbf{v} - \mathbf{v}^h)^2 \, dv \tag{32}$$

where $\mathbf{v}$ stands for the displacement $\mathbf{u}$, the temperature ϑ and the temporal variable z. This norm provides a measure of the space-time discretization error. Since the exact solution for the variables $\mathbf{u}$, ϑ and z is unknown we approximate $\mathbf{v}$ by the recovered gradient $\mathbf{v}^*$. The error norm for the temporal variable is related to the time step $\mathcal{I}_{n-1}$ since $\dot{z}^*$ cannot be computed in the current time step but only in the following increment.

Superconvergent Patch Recovery in $\mathcal{B}$. Within the subsets $\Omega_p^m \subset \Omega^m$ and $\Omega_p^\vartheta \subset \Omega^\vartheta$ (Fig. 3), referred to as the mechanical and thermal patch assembly, respectively, a simple polynomial expansion $\tau_i^*(\mathbf{x}) = \mathbf{p}(\mathbf{x})\,\mathbf{a}_i$ of each component of the improved gradients $\boldsymbol{\sigma}^*$ and $\mathbf{q}^*$, for simplicity denoted by $\boldsymbol{\tau}^*$, is applied. $\mathbf{p}$ represents an appropriate polynomial basis, and $\mathbf{a}_i$ is a set of unknown parameters. In general the subsets Ω_p^m and Ω_p^ϑ do not coincide

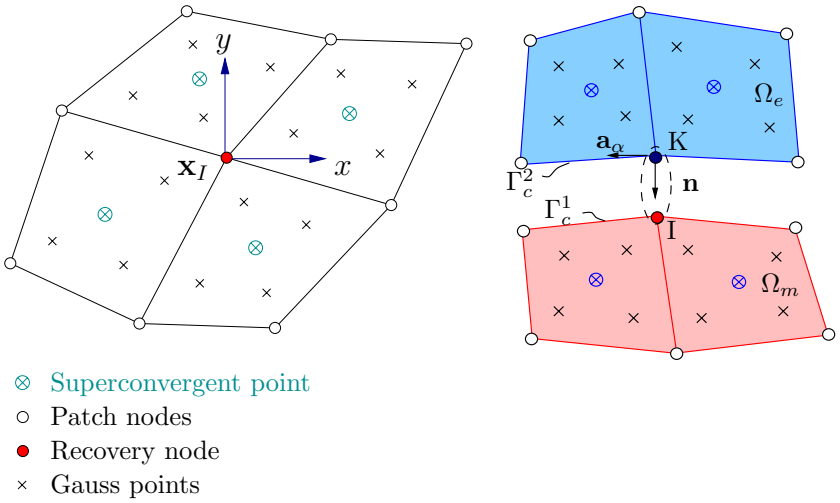

Figure 4: Patch assemblies

essentially. For simplicity Ω_p refers to an arbitrary subset of the thermal or the mechanical grid in the following.
A least-square-fit minimization leads to the linear equation system

$$\int_{\Omega_p} \mathbf{p}^T \mathbf{p}\, d\Omega\, \mathbf{a}_i = \int_{\Omega_p} \mathbf{p}\, \tau_i^h\, d\Omega \tag{33}$$

which has to be solved for every gradient component i. The nodal values at the recovery node in the center of the patch are simply given by $\tau_{iI}^* = \tau_i^*(\mathbf{x}_I) = \mathbf{p}(\mathbf{x}_I)\, \mathbf{a}_i$.
Superconvergent Patch Recovery on $\partial\mathcal{B}_c$. The recovery algorithm on the boundary can be improved substantially by taking into account the boundary conditions, as shown in (Wiberg et al., 1998). An analogous approach is applied here to derive improved gradients at the contact boundary. For this purpose, we search for the closest slave node I on Γ_c^m related to a the master node K of Γ_c^2, see Fig. 4 right. A patch of elements surrounding node K defines the standard patch Ω_s and the set of elements surrounding node I is henceforth referred to as extended patch Ω_e. According to the principle of *actio et reactio* on the contact boundary we require the improved stresses to be continuous across the interface

$$[\![t_N^*]\!] = 0 \quad , \quad [\![t_{T\alpha}^*]\!] = 0 \qquad \text{on } \Gamma_c \tag{34}$$

The principle of conservation of energy requires the influx of heat due to conduction q_{hc} from one side of the contact boundary to be equal and that of the opposite side. Hence we can formulate the requirement $[\![q_{hc}^*]\!] = 0$ and with (16) for the total heat flux

$$[\![\mathbf{q}^* \cdot \mathbf{n}]\!] = -d_{fric} \quad \text{on } \Gamma_c \tag{35}$$

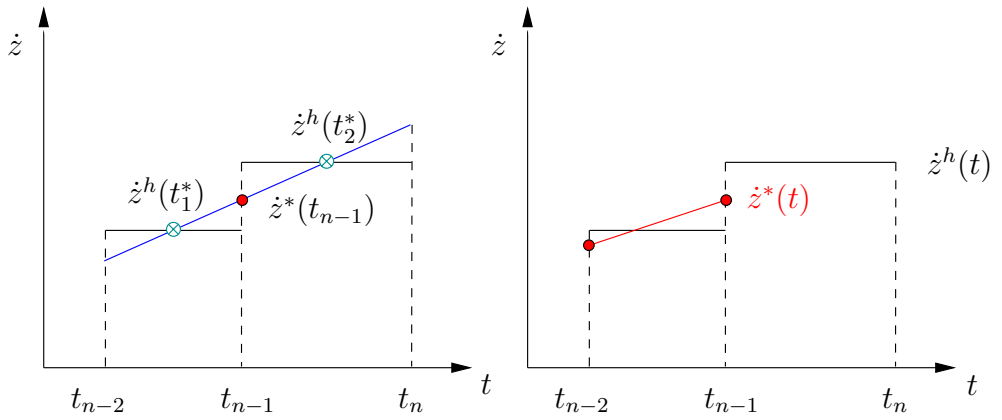

Figure 5: Time patch (left) and time-discretization error (right)

In each sub domain Ω^s and Ω^e a polynomial expansion $\boldsymbol{\sigma}_s^* = \mathbf{P}_s^\sigma \cdot \mathbf{a}_s^\sigma$ and $\boldsymbol{\sigma}_e^* = \mathbf{P}_e^\sigma \cdot \mathbf{a}_e^\sigma$ is performed for the complete stress tensor. In the same way the expansion $\mathbf{q}_s^* = \mathbf{P}_s^q \cdot \mathbf{a}_s^q$ and $\mathbf{q}_e^* = \mathbf{P}_e^q \cdot \mathbf{a}_e^q$ of the complete heat flux vector is given.
The unconstraint minimization problems for stresses and heat flux are

$$\int_{\Omega^s} (\boldsymbol{\tau}_s^h - \boldsymbol{\tau}_s^*)^2 \, d\Omega + \int_{\Omega^e} (\boldsymbol{\tau}_e^h - \boldsymbol{\tau}_e^*)^2 \, d\Omega \longrightarrow MIN \tag{36}$$

where the indices s and e denote values in the standard and the extended patch, respectively. The continuity requirements (34) and (35) are enforced by penalty functionals included in (36). This leads to an extended minimization problem which yields two linear equation systems that are coupled in the unknowns $\mathbf{a}_e^\sigma$, $\mathbf{a}_e^\sigma$ and $\mathbf{a}_e^q$, $\mathbf{a}_e^q$, respectively.

Superconvergent patch recovery in time Within the patch of two time steps $\mathcal{T}_{n-1} \cup \mathcal{T}_n$ (see Fig. 5) we apply a linear polynomial expansion of the improved time gradient $\dot{z}^*$:

$$\dot{z}^*(t) := \mathbf{p}_\tau(t) \cdot \mathbf{a}_\tau \quad \text{mit} \quad \mathbf{p}_\tau(t) = [\,1\,,\,t\,] \tag{37}$$

The least square fit minimization

$$\int_{\mathcal{T}_{n-1} \cup \mathcal{T}_n} [\,\dot{z}^h(t^*) - \dot{z}^*(t)\,]^2 \, dt \to MIN \tag{38}$$

with the superconvergent time-points

$$t_1^* = \frac{1}{2}\,[t_{n-1} + t_{n-2}] \quad \text{bzw.} \quad t_2^* = \frac{1}{2}\,[t_n + t_{n-1}] \quad .$$

leads to the linear equation system

$$\int_{\mathcal{T}_{n-1}\cup\mathcal{T}_n} \mathbf{p}_\tau \otimes \mathbf{p}_\tau \, dt \cdot \mathbf{a}_\tau = \int_{\mathcal{T}_{n-1}\cup\mathcal{T}_n} \mathbf{p}_\tau \, \dot{z}^h \, dt \tag{39}$$

with its solution $\mathbf{a}_\tau$.

2.5 Space-time adaptive strategy

As discussed before, we will state the adaptive method as a nonlinear optimization problem: construct a spatial $\mathbf{u}$-mesh or θ-mesh and a temporal z-mesh such that the associated FEM-solutions satisfy

$$\eta_v = \frac{||\nabla \mathbf{e}_v||^2_{L2(\Omega^u)}}{||\nabla \mathbf{e}_v||^2_{L2(\Omega^u)} + ||\nabla \mathbf{v}^h||^2_{L2(\Omega^v)}} \leq \eta_v^{Tol} \tag{40}$$

where v stands for the displacement $\mathbf{u}$, the temperature θ and the time variable z. η_v is the relative error in the space time mesh and η_v^{Tol} is a given tolerance. Furthermore we require the space-time meshes to be optimal in the sense that the element error is equally distributed between all n_{el}^v elements in the specific mesh. This yields to local predicted new element sizes

$$h^v_{new} = h^v_{old} \left(\frac{\bar{e}_v}{||\nabla \mathbf{e}_v||_{L2(\Omega_T)}} \right)^{\frac{1}{p}} \tag{41}$$

where p is the polynomial order. The new mesh is generated by the advancing front method, but also different techniques can be applied.

Note that we have to re-compute the time step $\mathcal{T}_{n-1}$ if condition the error indicator predicts a change in time step.

2.6 Numerical example

As an example we consider a rubber tire which is loaded by an internal pressure p_i and by a vertical force of $2F_v$. For simplicity the tire is modelled without the belt, bead apex core and rim flange. The material data of the tire and the ground are stated in Table 1. The real contact situation on the rim flange is replaced by a prescribed velocity $\bar{v}$, which forces the tire to a tangential movement. The rim flange and the lower end of the ground have a prescribed relative temperature of $\bar{\vartheta} = 0K$. All other boundaries with exception of the contact zone are supposed to have adiabatic conditions.
After a phase of sticking the tire slides tangentially over the ground and is heated due to frictional dissipation in the contact zone. At the end of the sliding movement the tire shifts back elastically to its final position. The path of movement is schematically depicted in Fig. 7. The adaptive algorithm

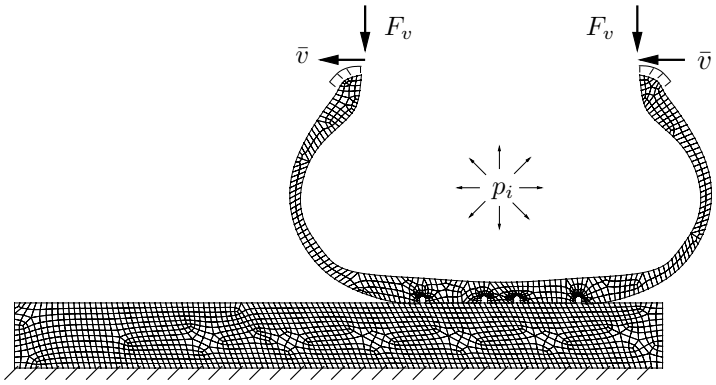

Figure 6: Initial mesh and loads

	Tire	Ground
Bulk modulus K	$333\ N/mm^2$	$3333\ N/mm^2$
Shear modulus μ	$35\ N/mm^2$	$3846\ N/mm^2$
Thermal expansion α	$0.1 \cdot 10^{-3}\ K^{-1}$	$0.1 \cdot 10^{-4}\ K^{-1}$
Thermal conductivity k	$0.2\ N/sK$	$0.2\ N/sK$
Heat capacity c_p	$0.2 \cdot 10^{-3}\ mm^2/s^2K$	$0.4 \cdot 10^{-3}\ mm^2/s^2K$
Density ρ_0	$1.0 \cdot 10^{-9}\ Ns^2/mm^4$	$3.0 \cdot 10^{-9}\ Ns^2/mm^4$
Friction coefficient μ	0.4	
Parameter h_{c0}	$150\ N/sK$	
Hardness H_v	$100\ N/mm^2$	
Parameter ϵ	1.5	

Table 1: Material- and Interfacial Data

starts for the mechanical subproblem with a prescribed relative error tolerance of $\bar{\eta}_u := 15\%$ at $t = t_1$. The thermal sub-problem is solved not until $t = t_2$ with a given error tolerance of $\bar{\eta}_\theta := 15\%$ since frictional heating is initiated not until $t = t_2$. Figures 8 and 9 depict the indicated relative error of both sub-solutions. Once the prescribed tolerance is exceeded for one sub-problem a new adapted mesh is generated. Exemplary some adapted meshes are depicted in Fig. 10. We observe a significant grid condensation in both, the mechanical and thermal mesh evolution, due to the complex solution gradient starting from the contact area, see temperature field and effective heat flux $q_{eff} := \sqrt{q_i\, q_i}$ in Fig. 11. Nevertheless the global progressive mesh optimization for both subproblems develops quite different, although the error tolerances are identical.

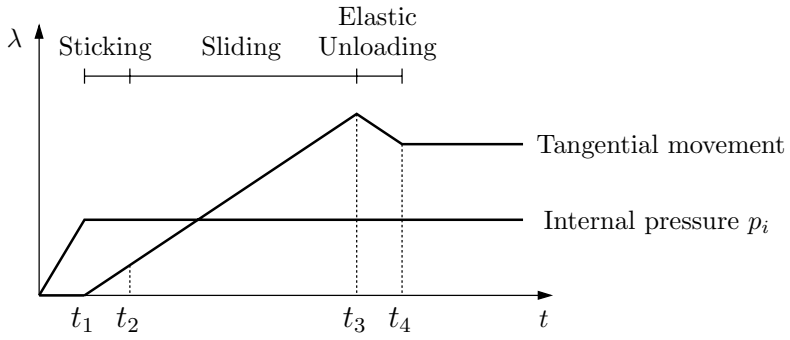

Figure 7: Load-Path internal pressure and tangential movement

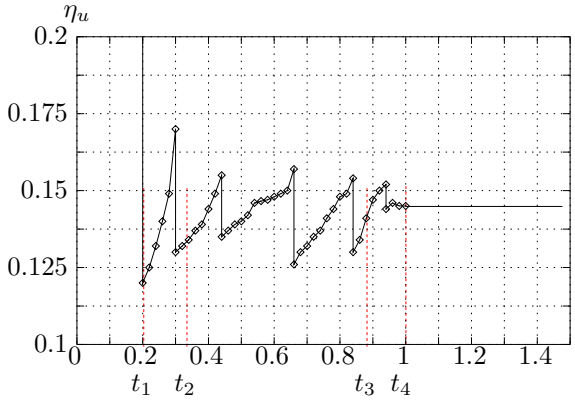

Figure 8: Indicated relative error η_u

References

Armero, F. and Simo, J. (1992). A new unconditionally stable fractional step method for non–linear coupled thermomechanical problems. *International Journal for Numerical Methods in Engineering*, 35:737–766.

Bernadi, C., Maday, Y., and Patera, A. (1994). A new nonconforming approach to domain decomposition: the motar element method. In Brezis, H. and Lions, J. L., editors, *Nonlinear Partial Differential Equations and their Application*. Pitman.

Betsch, P. and Steinmann, P. (2001). Conservation properties of a time fe method–part ii: Time-stepping schemes for non-linear elastodynamics. *Int. J. Num. Meth. Engng.*, 50:1931–1955.

de Saracibar, C. A. (1998). Numerical analysis of coupled thermomechanical frictional

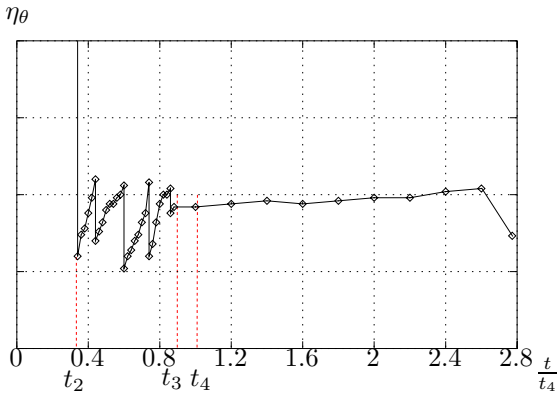

Figure 9: Indicated relative error η_θ

contact problems. computational model and applications. *Archives of Computational Methods in Engineering*, 5:243–301.

El-Abbasi, N. and Bathe, K.-J. (2001). Stability and patch test performance of contact discretizations and a new solution algorithm. *Computers and Structures*, 79:1473–1486.

Hulme, B. (1972). One-step piecewise polynomial galerkin methods for initial value problems. *Mathematics of Computation*, 26:415–426.

Johnson, C. and Hansbo, P. (1992). Adaptive finite element methods in computational mechanics. *Computer Methods in Applied Mechanics and Engineering*, 101:143–181.

Krause, R. H. and Wohlmuth, B. I. (2001). A dirichlet–neumann type algorithm for contact problems with friction. *FU-Berlin, Preprint A-01-09*, pages 1–16.

Luenberger, D. G. (1984). *Linear and Nonlinear Programming*. Addison-Wesley, Reading.

McDevitt, T. W. and Laursen, T. A. (2000). A mortar-finite element formulation for frictional contact problems. *International Journal for Numerical Methods in Engineering*, 48:1525–1547.

Miehe, C. (1988). *Zur numerischen Behandlung thermomechanischer Prozesse*. PhD thesis, Institute for Structural and Numerical Mechanics, University of Hannover.

Papadopoulos, P. and Taylor, R. L. (1992). A mixed formulation for the finite element solution of contact problems. *Computer Methods in Applied Mechanics and Engineering*, 94:373–389.

Rebel, G., Park, K. C., and Felippa, C. A. (2000). A ccontact-impact formulation based on localised lagrange multipliers. Technical Report CU-CAS-00-18, College of Engineering at University of Colorado, Bolder, Colorado 80309.

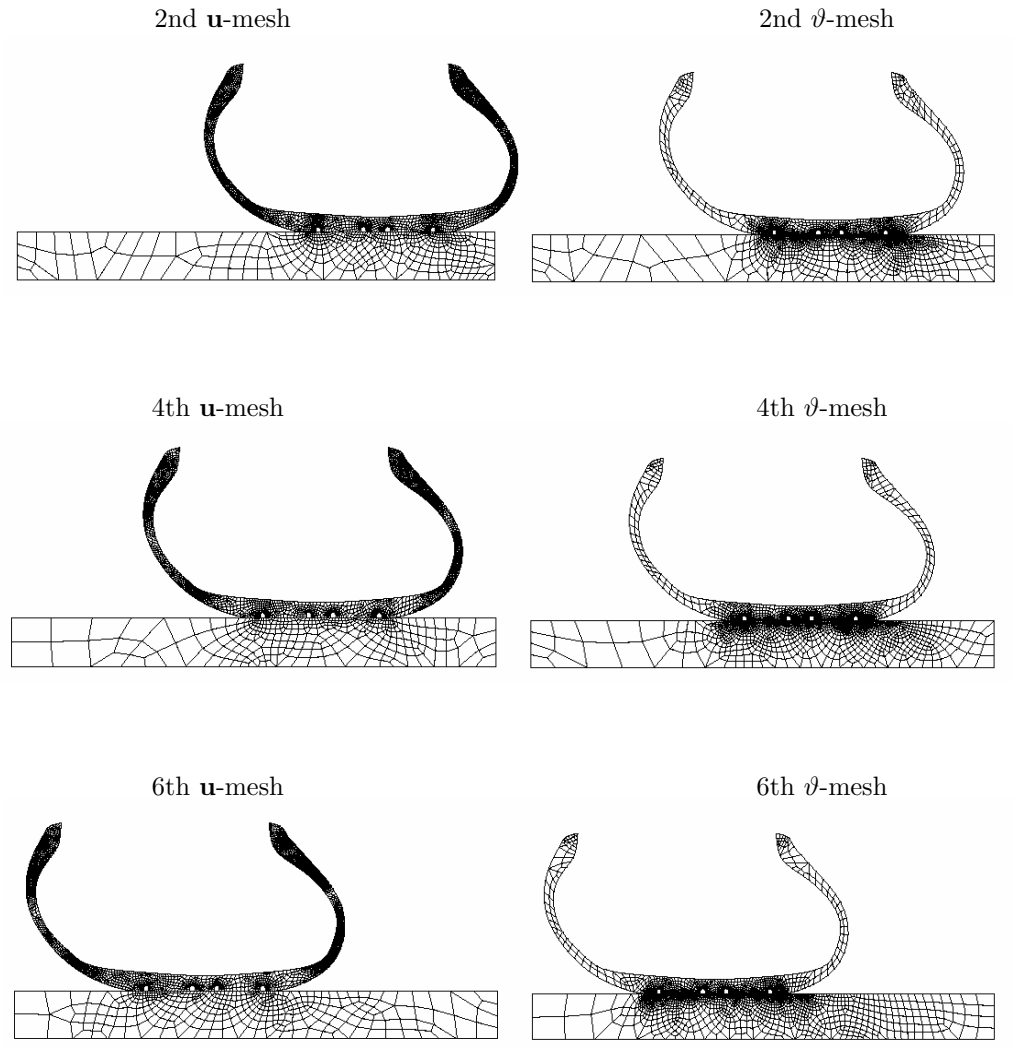

Figure 10: Evolution of adapted mechanical and thermal meshes

Simo, J. C., Wriggers, P., and Taylor, R. L. (1985). A perturbed Lagrangian formulation for the finite element solution of contact problems. *Computer Methods in Applied Mechanics and Engineering*, 50:163–180.

Wiberg, N.-E., Abdulwahab, F., and Ziukas, S. (1998). Enhanced superconvergent patch recovery incorporating equilibrium and boundary conditions. *International Journal for Numerical Methods in Engineering*, 37:3417–3440.

Wohlmuth, B. I. (2000a). *Discretization Methods and Iterative Solvers based on Domain Decomposition*. Springer Verlag, Berlin, Heidelberg, New York.

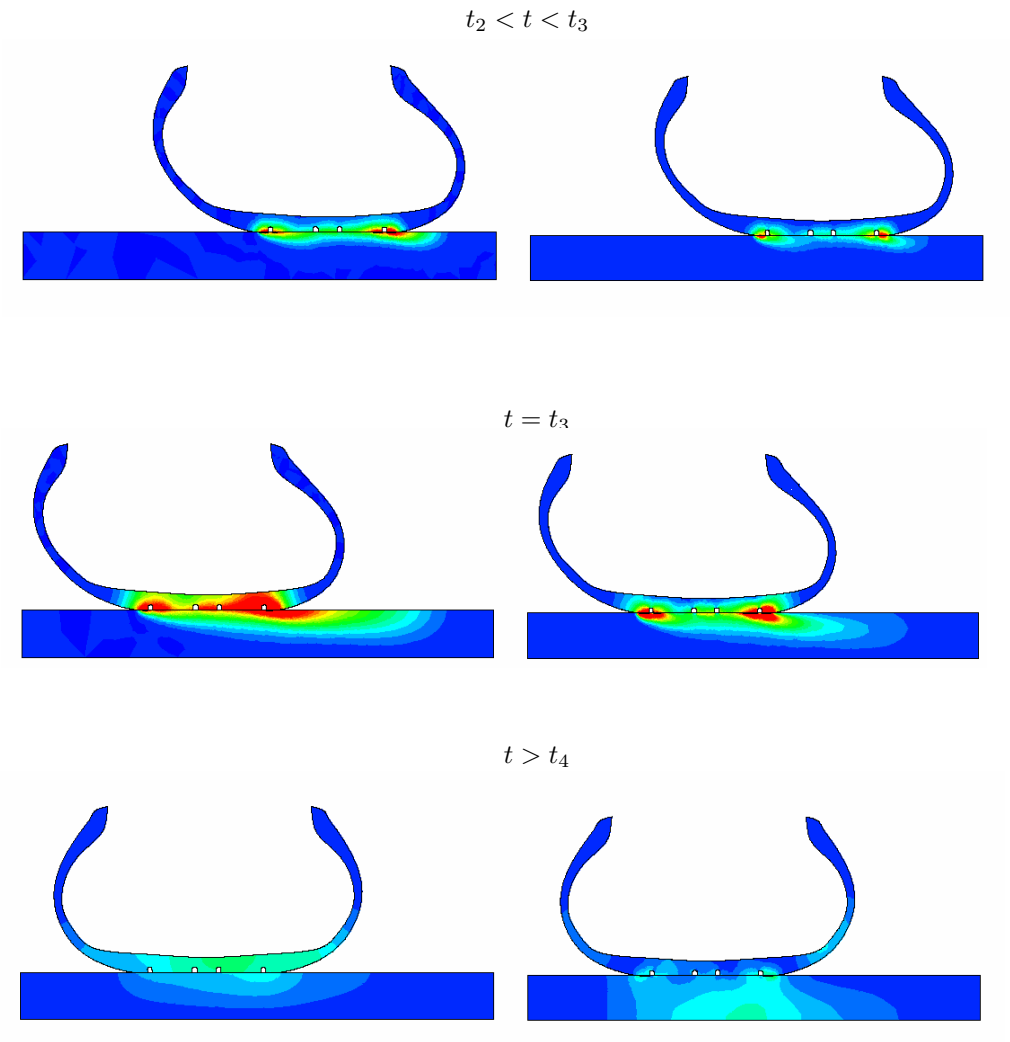

Figure 11: Temperature (left) und effective heat flux q_{eff} (right)

Wohlmuth, B. I. (2000b). A mortar finite element method using dual spaces for the lagrange multiplier. *SIAM, Journal of Numerical Analysis*, 38:989–1012.

Wriggers, P. (1987). On consistent tangent matrices for frictional contact problems. *Proceedings of NUMETA 87, eds.: Pande, G.N. , Middleton J.*

Wriggers, P. (2002). *Computational Contact Mechanics*. Wiley, Chichester.

Wriggers, P. and Miehe, C. (1994). Contact constraints within coupled thermomechanical analysis - a finite element model. *Computer Methods in Applied Mechanics and Engineering*, 113:301–319.

Zienkiewicz, O. and Zhu, J. Z. (1987). A simple error estimator and adaptive procedure for practical engineering analysis. *Int. J. Num. Meth. Engng.*, 24:337–357.